NASA/TM—2008-214406 ARL–TR–0646

Impact Resistance of EBC Coated SiC/SiC Composites

Ramakrishna T. Bhatt
U.S. Army Research Laboratory, Glenn Research Center, Cleveland, Ohio

Sung R. Choi
Naval Air Systems Command, Patuxent River, Maryland

Laura M. Cosgriff
Cleveland State University, Cleveland, Ohio

Dennis S. Fox
Glenn Research Center, Cleveland, Ohio

Kang N. Lee
Rolls-Royce Corporation, Indianapolis, Indiana

October 2008

NASA STI Program . . . in Profile

Since its founding, NASA has been dedicated to the advancement of aeronautics and space science. The NASA Scientific and Technical Information (STI) program plays a key part in helping NASA maintain this important role.

The NASA STI Program operates under the auspices of the Agency Chief Information Officer. It collects, organizes, provides for archiving, and disseminates NASA's STI. The NASA STI program provides access to the NASA Aeronautics and Space Database and its public interface, the NASA Technical Reports Server, thus providing one of the largest collections of aeronautical and space science STI in the world. Results are published in both non-NASA channels and by NASA in the NASA STI Report Series, which includes the following report types:

- TECHNICAL PUBLICATION. Reports of completed research or a major significant phase of research that present the results of NASA programs and include extensive data or theoretical analysis. Includes compilations of significant scientific and technical data and information deemed to be of continuing reference value. NASA counterpart of peer-reviewed formal professional papers but has less stringent limitations on manuscript length and extent of graphic presentations.

- TECHNICAL MEMORANDUM. Scientific and technical findings that are preliminary or of specialized interest, e.g., quick release reports, working papers, and bibliographies that contain minimal annotation. Does not contain extensive analysis.

- CONTRACTOR REPORT. Scientific and technical findings by NASA-sponsored contractors and grantees.

- CONFERENCE PUBLICATION. Collected papers from scientific and technical conferences, symposia, seminars, or other meetings sponsored or cosponsored by NASA.

- SPECIAL PUBLICATION. Scientific, technical, or historical information from NASA programs, projects, and missions, often concerned with subjects having substantial public interest.

- TECHNICAL TRANSLATION. English-language translations of foreign scientific and technical material pertinent to NASA's mission.

Specialized services also include creating custom thesauri, building customized databases, organizing and publishing research results.

For more information about the NASA STI program, see the following:

- Access the NASA STI program home page at *http://www.sti.nasa.gov*

- E-mail your question via the Internet to *help@sti.nasa.gov*

- Fax your question to the NASA STI Help Desk at 301–621–0134

- Telephone the NASA STI Help Desk at 301–621–0390

- Write to:
  NASA Center for AeroSpace Information (CASI)
  7115 Standard Drive
  Hanover, MD 21076–1320

NASA/TM—2008-214406 ARL–TR–0646

Impact Resistance of EBC Coated SiC/SiC Composites

Ramakrishna T. Bhatt
U.S. Army Research Laboratory, Glenn Research Center, Cleveland, Ohio

Sung R. Choi
Naval Air Systems Command, Patuxent River, Maryland

Laura M. Cosgriff
Cleveland State University, Cleveland, Ohio

Dennis S. Fox
Glenn Research Center, Cleveland, Ohio

Kang N. Lee
Rolls-Royce Corporation, Indianapolis, Indiana

National Aeronautics and
Space Administration

Glenn Research Center
Cleveland, Ohio 44135

October 2008

This work was sponsored by the Fundamental Aeronautics Program at the NASA Glenn Research Center.

Level of Review: This material has been technically reviewed by technical management.

Available from

NASA Center for Aerospace Information
7115 Standard Drive
Hanover, MD 21076–1320

National Technical Information Service
5285 Port Royal Road
Springfield, VA 22161

Impact Resistance of EBC Coated SiC/SiC Composites

Ramakrishna T. Bhatt
U.S. Army Research Laboratory
Glenn Research Center
Cleveland, Ohio 44135

Sung R. Choi
Naval Air Systems Command
Patuxent River, Maryland 20670

Laura M. Cosgriff
Cleveland State University
Cleveland, Ohio 44115

Dennis S. Fox
National Aeronautics and Space Administration
Glenn Research Center
Cleveland, Ohio 44135

Kang N. Lee
Rolls-Royce Corporation
Indianapolis, Indiana 46206

Abstract

Impact performance of 2-D woven SiC/SiC composites coated with 225 and 525 µm thick environmental barrier coating (EBC) was investigated. The composites were fabricated by melt infiltration and the EBC was deposited by plasma spray. Impact tests were conducted at room temperature and at 1316 °C in air using 1.59-mm diameter steel-balls at projectile velocities ranging from 110 to 375 m/s. Both microscopy and nondestructive evaluation (NDE) methods were used to determine the extent of damage in the substrate and coating with increasing projectile velocity. The impacted specimens were tensile tested at room temperature to determine their residual mechanical properties. At projectile velocities less than 125 m/s, no detectable damage was noticed in the MI SiC/SiC composites coated with 525 µm EBC. With increase in projectile velocity beyond this value, spallation of EBC layers, delamination of fiber plies, and fiber fracture were detected. At a fixed projectile velocity, the composites coated with 525 µm EBC showed less damage than the composite coated with 225 µm EBC. Both types of EBC coated composites retained a large fraction of the baseline properties of as-fabricated composites and exhibited non-brittle failure after impact testing at projectile velocities up to 375 m/s. Exposure of impact tested specimens in a moisture environment at 1316 °C for 500 hr indicated that the through-the-thickness cracks in the EBC coating and delamination cracks in the substrate generated after impact testing acted as conduits for internal oxidation.

1. Introduction

SiC fiber reinforced SiC matrix composites (SiC/SiC) are candidate materials for next generation aerospace, power, and nuclear applications because of their high temperature strength, high creep resistance, and high thermal conductivity. Currently these composites are fabricated by three processing approaches: melt infiltration (MI), chemical vapor infiltration (CVI), polymer infiltration and pyrolysis (PIP). To date the SiC/SiC composites fabricated by MI and by CVI are investigated the most (ref. 1).

Studies have shown that all three types of SiC/SiC composites are stable up to 1300 °C in air or in oxidizing environments after extended exposure times, predominantly due to growth of adherent, protective silica scale on the external surfaces (refs. 2 and 3). In contrast, in a combustion environment containing moisture, these composites exhibit recession due to simultaneous formation and volatilization of silica at temperatures greater than 1100 °C (refs. 4 and 5). To protect these composites from surface recession environmental barrier coatings (EBC) have been developed, key examples of which are multilayered coatings having a barium strontium aluminum silicate (BSAS) and rare earth silicate top coat (refs. 6 and 7). The BSAS and rare earth silicate based EBCs have upper temperature capabilities of ~1316 °C (ref. 7) and ~1482 °C (ref. 8), respectively for applications over thousands of hours. Flat coupons and sub-elements of MI SiC/SiC composites coated with BSAS based EBC coating have been investigated under engine exposure conditions for strength and microstructural stability at temperatures to 1300 °C (refs. 9 and 10). Also, durability of a MI SiC/SiC composite combustor liner coated with the BSAS based EBC has been demonstrated in an industrial scale engine ~1200 °C for up to 14,000 hr (ref. 11). However, long term durability of EBC coated MI SiC/SiC composite components such as nozzle vanes and blades, in the flow path of the combustion gases has not been fully investigated. In the flow path of a typical turbine, the combustions gases are traveling at velocities as high as 600 m/s (ref. 12). Any objects that enter the turbine inlet are carried by the combustion gases and impact the components. A wide variety of particles and objects can be ingested into the turbine engines depending on the operating conditions. In commercial aero-derivative engines, small objects such as rivets, solder, spalled coatings, ice particles and coke clinkers and large objects such as ice slabs and birds commonly enter into the gas stream. In addition to the above objects, sand and salt are the most common objects in military engines. Single small object impact can cause local damage to the EBC coatings and substrate, whereas single large object impact can lead to failure of the component. In contrast, multiple small particle impacts that occur from sand erode the coatings as well as substrate of the components.

In the current engines, the metal components are coated with a thermal barrier coating to keep the substrate temperature below the design allowable. The TBC coating serves as an insulating layer between the substrate and the hot gases, reducing the substrate temperature substantially, and increasing life of the components. However, the design life of the components is based on life of the uncoated metal under the operating conditions of the engines. In other words the component substrate is prime reliant, not the TBC coating. Under the operating conditions of the engines, the TBC may get embedded into the substrate due to impact or locally spall off due to thermal cycling, causing hot spots (refs. 13 and 14). Effects of hot spots on the long term durability are accounted for in the design allowable. In addition, the impact of small hard objects on components causes local damage but not complete failure because of the compliant nature of the substrate material. Oxygen in the combustion environment oxidizes the metallic components resulting in growth of oxide scale on their external surfaces. However the influence of moisture in the combustion environment on the oxide scale growth has not been fully understood. Also there is no evidence of adverse effects of oxide scale growth on the aero performance, life and thermo-mechanical properties of the components. On the other hand sand erosion and corrosion due to deposition of salt and siliceous material severely degrade the life of the components. Therefore erosion and corrosion are major issues in the current engines compared to local loss of TBC or oxidation due to moisture in the combustion environments.

In contrast, fiber-reinforced composites are not as compliant as metals and require reliable EBC coating to operate at temperatures greater than 1100 °C. Without an EBC coating the substrate material does not have adequate life. In other words the EBC coating should be prime reliant if SiC/SiC composites were to be used for hot section components. This is a drastically different design philosophy compared to the current metallic components. In addition, for successful use of SiC/SiC composites in hot sections of the turbines, the EBC coating should serve several functions, besides protecting the substrate from surface recession such as impact resistance, and erosion and corrosion resistance while not adversely affecting strength of the substrate.

The objectives of this study are to determine impact resistance of EBC coating, evaluate the influence of EBC coating thickness on impact resistance, to study the influence of impact damage on in-plane tensile properties, and to determine consequences of impact damage on internal oxidation. The impact resistance of uncoated MI SiC/SiC composites is addressed in a companion paper.

2. Experimental Procedure

The MI SiC/SiC composite panels, ~230- (L) by 150- (W) by 2.4-mm (T), were purchased from GE Composite Ceramic Products (GECCP), Newark, Delaware. The composites were fabricated by infiltrating SiC particle slurry into a porous SiC/SiC preform and then filling the remaining porosity with molten silicon. The processing details can be found in reference 15. The composite consists of 8 layers of 2-D woven 5HS Sylramic-iBN SiC fibers cloth in a complex SiC matrix which is a mixture of chemically vapor deposited SiC matrix, SiC particles and silicon metal. The as-fabricated SiC/SiC composites contained ~34 vol% SiC fibers, ~5 vol% BN coating, and ~58 vol% SiC coating, SiC particles and silicon, and ~3 vol% porosity.

The as-fabricated composite panels were machined into flexure specimens of dimensions 45- (L), 8- (W), and 2.2 to 2.4-mm (T) and tensile dog-boned specimens of dimensions 152- (L), 13- (W), and 2.2 to 2.4-mm (T) with a reduced gage section using diamond impregnated metal bonded cut-off wheels and a sonic mill.

For better adherence of the EBC coating, the gage section of the tensile specimens was first grit blasted with ~35 μm Al_2O_3 particles and then coated with a multilayered EBC coating by atmospheric pressure plasma spraying. Although not reported here, we did not observe any significant loss of in-plane properties of MI SiC/SiC composites due to grit blasting. The reference 16 describes details of the plasma spray deposition technique. Briefly, plasma spraying (PS) is a high velocity impact deposition process in which melting, quenching, and consolidation take place in a single step. In this process PS grade ceramic or metal powder is injected radially in the direction of a high velocity and high temperature plasma flow. Molten drops of powder are produced, which are propelled rapidly toward a substrate by the plasma flow and the high-velocity carrier gas. Upon impingement on the substrate, the drops are quenched and solidified. Coatings of desired thickness are produced by successive impingement of drops referred to as “splats” on the substrate. The EBC coating consists of three sub layers: first a bond coat layer of silicon was deposited on top of the substrate followed by an intermediate mixed layer of mullite + barium strontium aluminum silicate (BSAS), and then by a top layer of BSAS. Two different coating thicknesses namely, ~75 μm silicon/~75 μm mullite + BSAS/~75 μm BSAS and ~125 μm silicon/~200 μm mullite + BSAS/~200 μm BSAS were investigated. Hence forth the 75/75/75 combination is referred to as the 225 μm coating and the 125/200/200 combination is referred to as the 525 μm coating. The 225 μm coating is typically deposited on turbine nozzle vanes and blades, and the 525 μm coating on combustor liners.

Impact tests were performed with a gas gun that accelerated a single solid sphere of hardened steel onto the EBC coated surfaces of dog-boned tensile specimens at normal incidence (ref. 17). The specimens were held at their ends in a “C” shaped clamp. For high temperature impact testing, the gage section of the specimen was heated by an atmospheric pressure burner rig. In both test configurations, the specimens were impacted with hardened (HRC≥60) chrome steel-balls (diameter ~1.59-mm, density 7.8 gm/cc) at velocities ranging from 110 to 400 m/s. At each test condition only one specimen was tested. The extent of target specimen damage with increasing projectile velocity was imaged by optical microscopy, scanning electron microscopy (SEM), computed tomography (CT), and pulsed thermography (PT). Pulsed thermography is a full field non-destructive evaluation (NDE) technique for detecting subsurface flaws and material variations. An infrared camera monitors the cooling behavior of a component after the surface is heated with an instantaneous pulse of heat generated by 2 xenon flash lamps. The heat is absorbed at the surface and flows toward the backside of the material. Disruptions in heat flow, due to subsurface discontinuities, results in localized surface temperature variations which are detected with an infrared camera (ref. 18). The micro-focus CT system is a radiographic technique that provides a cross-sectional view of a component. The CT imaging procedures similar to that described in reference 19 were used.

2.1 Post-Impact Strength Testing

For tensile testing, each impact tested dog-bone specimen was loaded in a servo-hydraulic test frame equipped with self-aligning grips, and a spring-loaded clip-on gauge was attached to the 25-mm long straight section of the dog-boned specimen to monitor the displacement. The specimens were tested at room temperature and at 1316 °C until failure at a crosshead speed of 1.3 mm/min. One specimen was tested for each exposure condition. The tensile stress is calculated based on the cross-sectional area of the substrate and the EBC coating thickness is not considered in the calculations. This is a valid assumption because of low modulus of EBC coating.

3. Results

A SEM photograph of a typical cross section of a MI SiC/SiC composite specimen coated with plasma sprayed EBC is shown in figure 1. As described earlier the EBC coating consists of three sub-layers. The grayish layer on top of the substrate is the silicon layer. The intermediate layer is a mixture of mullite and BSAS. The top whitish layer is the BSAS. All sub layers contained numerous defects such as pores, and micro-cracks; but, none of the cracks propagated through the thickness of the coating. The coating thickness varies by ~10 percent with an inhomogeneous microstructure.

The EBC coated MI SiC/SiC specimens were impact tested at ambient temperature and at 1316 °C in air. In all cases only the side with EBC was impacted with the steel ball. This side is henceforth referred to as the impacted side. To distinguish pre existing defects from those produced after impact testing, the gage sections of each specimen were analyzed before and after impact testing by SEM, pulsed thermography and CT. Figure 2 shows the SEM micrographs of the gage section of the impacted specimen front (impacted) and back sides. The specimens had coating thickness of ~525 µm. The top half of the figure is the EBC coated side of the specimen, and appears white in the micrograph. The dark circles in the figure indicate the impacted zone. The bottom half of the figure is the backside of the specimen.

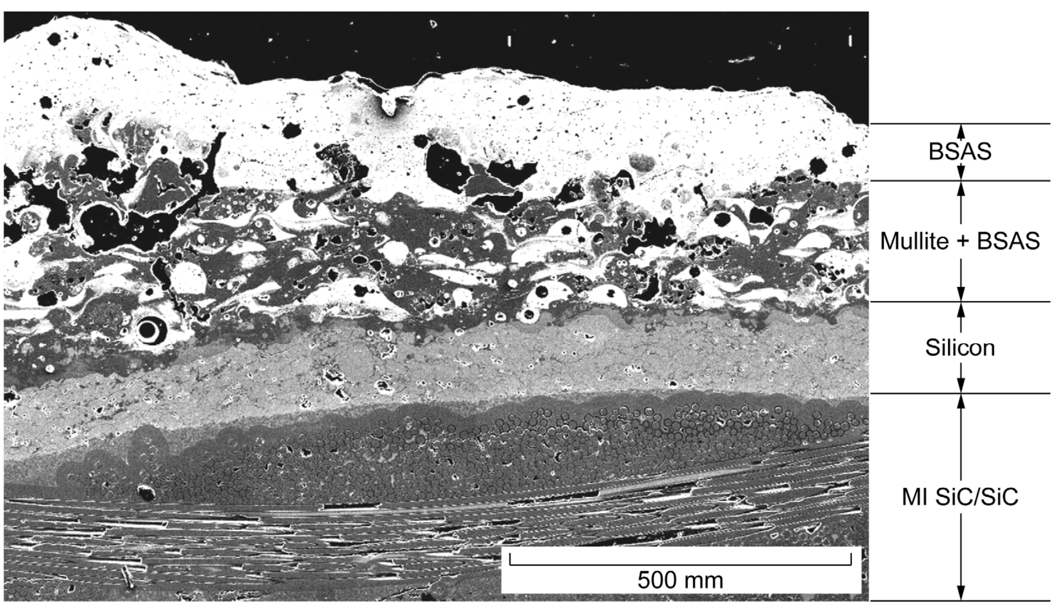

Figure 1.—SEM micrograph of typical cross section of plasma sprayed EBC coating on MI SiC/SiC substrate showing microstructure, composition and thickness of EBC sub-layers.

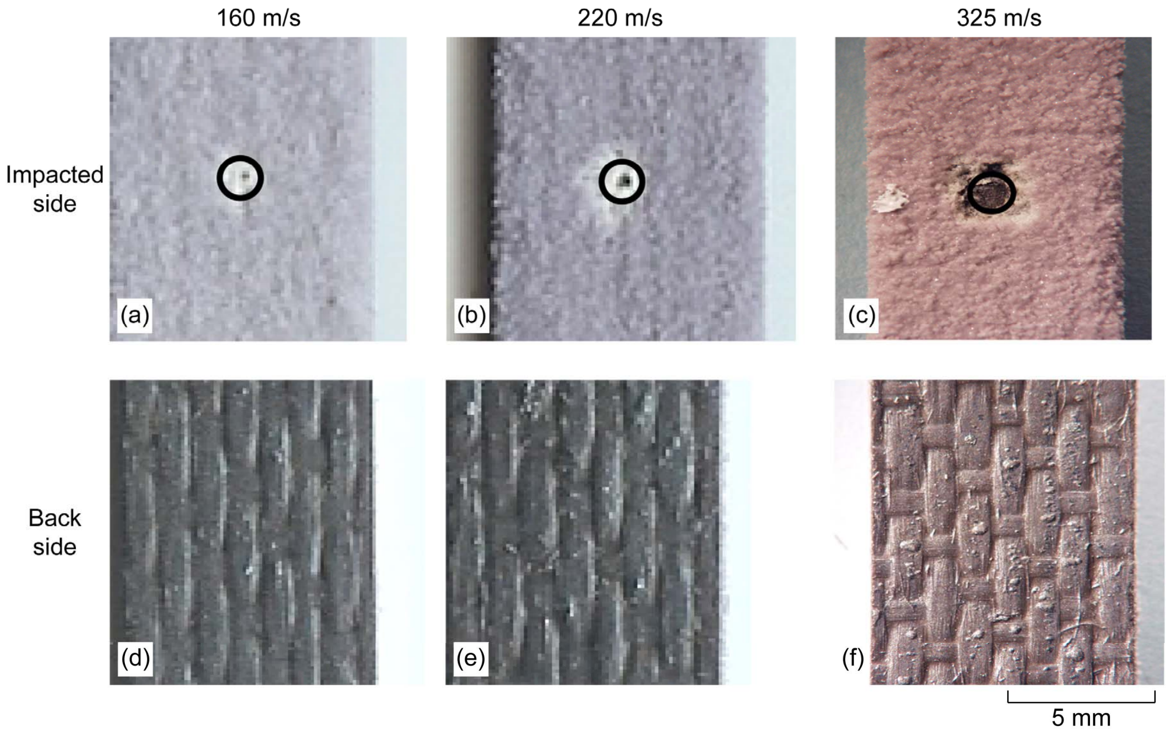

Figure 2.—Optical micrographs showing influence of projectile velocity on surface damage for 525 µm EBC coated MI SiC/SiC composites impact tested at room temperature.

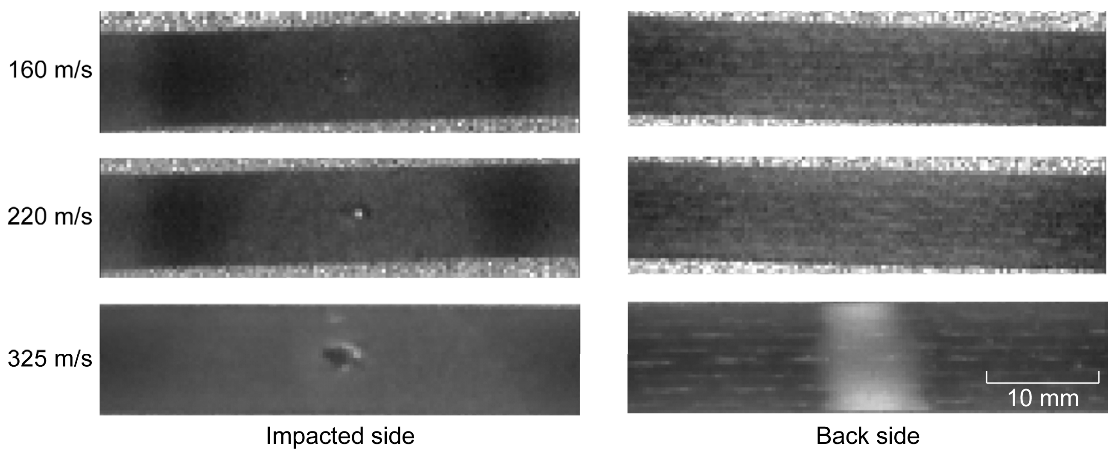

Figure 3.—Pulsed thermography images showing evolution of subsurface damage with projectile velocity for 525 µm EBC coated MI SiC/SiC composites impact tested at room temperature.

The weave pattern of the 2-D SiC cloth observed in figures 2(d), (e), and (f) also can be recognized in the thermal images shown in figure 3. At projectile velocities less than 220 m/s, little damage occurred to the EBC coating. With an increase in projectile velocity greater amounts of damage to EBC coating was noticed, but perforation or backside damage was not observed at projectile velocities as high as 375 m/s. In contrast, composite coated with 225 µm EBC showed increasing amount of backside damage at projectile velocities greater than 220 m/s and perforation at projectile velocities greater than 300 m/s.

Figures 3 and 4 show the thermal and CT images of the specimens shown in figure 2. These figures show both the surface and subsurface damages. The white spot at the center of the specimen in figure 3(c) is an indication of delamination area as detected from the backside of the sample with thermography. In the CT images shown in figure 4, defect identification in the substrate becomes more difficult because of

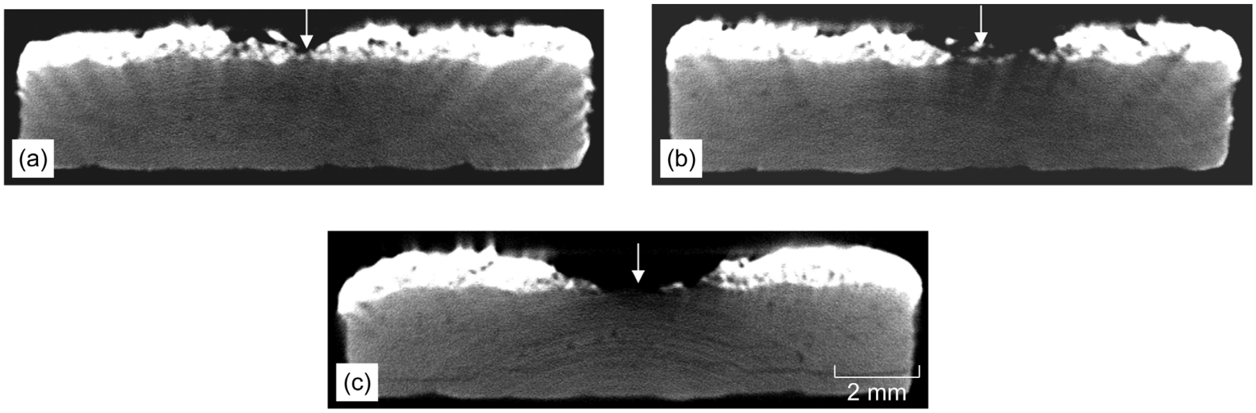

Figure 4.—CT images showing evolution of internal damage with projectile velocity for 525 μm EBC coated SiC/SiC composite specimens impact tested at room temperature. White arrows indicate impacted sites. (a) 160 m/s. (b) 220 m/s. (c) 325 m/s.

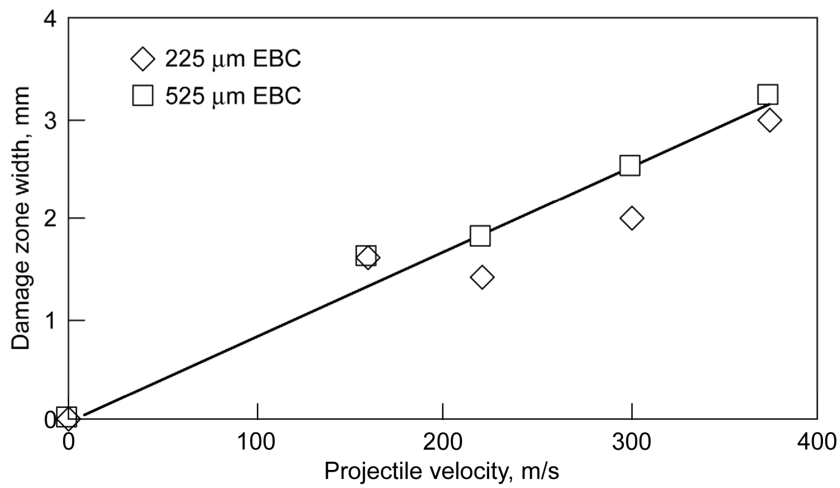

Figure 5.—Variation of impact damage zone width with projectile velocity for 525 μm EBC coated MI SiC/SiC composites impact tested at room temperature. Damage zone is analyzed by optical method.

different absorption rates of x-rays between the substrate and the EBC coating. This difference in absorption rates results as smearing in the images. The hemispherical rings in the CT images of figure 4 are also artifacts of the technique. However, using different exposure conditions and image enhancing techniques it is still possible to delineate and distinguish defects such as pores, fiber fracture, and delamination depending on the thickness of EBC coating and the substrate.

To determine the influence of EBC coating thickness, testing temperature, and projectile velocity on impact damage accumulation, the average width and depth of the impact crater created on the front side, and the average length of delamination cracks formed on the back side of the 225 and 525 μm EBC coated MI SiC/SiC composites impact tested at ambient temperature and at 1316 °C were measured from the optical micrographs, and the thermal and CT images. Figure 5 shows the maximum width of the impact crater measured from the optical photographs for the 225 and 525 μm EBC coated MI SiC/SiC composites impact tested at ambient temperature. It is obvious from the figure that as the projectile velocity is increased width of the damaged zone also increased linearly, but EBC coating thickness has limited influence on the damaged zone width because optical microscope detects only visible damage to the coating. Subsurface and internal damages can be identified with thermal and CT images.

Figures 6(a) and (b) show damaged zone width measured from the pulsed thermography data for the two EBC coated composites from the front and the back sides, respectively. Also included in figure 6(b) is the thermal data generated for the uncoated composites impact tested under similar conditions for comparison from reference 20. Figure 6(a) indicates that for the 225 μm EBC coated composites, the damage width initially increases with increase in projectile velocity up to a value of 250 m/s and then reaches a plateau which is equivalent to the width of the specimen. In contrast, the damaged zone width for the 525 μm EBC coated composites also increases with increase in projectile velocity, but the damaged zone width is considerably lower than that for the 225 μm EBC coated composites at comparable projectile velocity. On the back side of the composites, the damage behavior is similar to that in the front side, except that the extent of the damage is much greater than on the front side. For a fixed projectile velocity, two important conclusions can be derived from figure 6(b): first, the composites coated with thicker EBC show much smaller damage in the back side than those coated with thinner EBC; second, the extent of damage in uncoated composite is similar to that for the composite coated with 225 μm EBC. The last observation indicates thinner EBC coating is ineffective in reducing impact damage in components.

Impact test temperatures up to 1316 °C had no significant influence on impact behavior as illustrated by the extent of damage zone of EBC coated composites in figures 6 and 7. Therefore, thermal images or the plot of damage zone with projectile velocity for EBC coated composites impact tested 1316 °C are not shown.

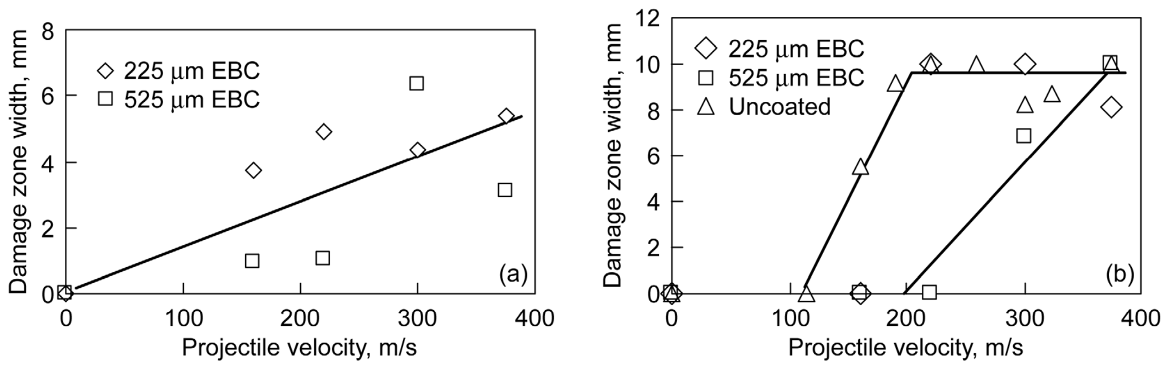

Figure 6.—Variation of impact damage zone width with projectile velocity for EBC coated MI SiC/SiC composites impact tested at room temperature. Damage zone is analyzed by pulsed thermography. Uncoated data is from reference 20. (a) Impacted side. (b) Back side.

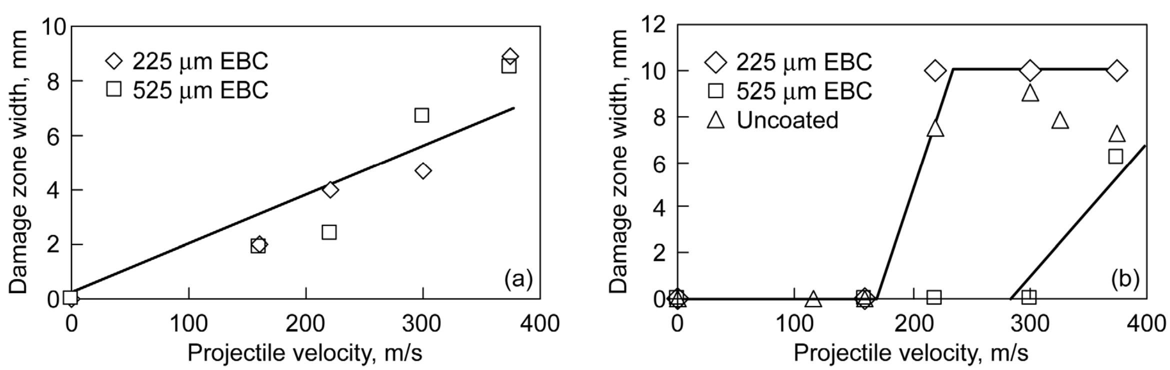

Figure 7.—Variation of impact damage zone width with projectile velocity for EBC coated MI SiC/SiC composites impact tested at 1316 °C in air. Damage zone is analyzed by pulsed thermography. Uncoated data is from reference 20. (a) Impacted side. (b) Back side.

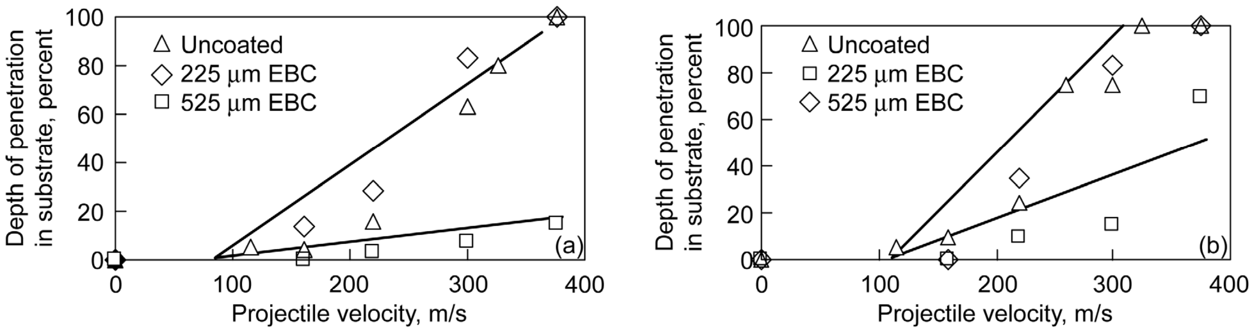

Figure 8.—Variation of impact damage depth with projectile velocity for EBC coated MISiC/SiC composites impact tested in air. Damage zone is analyzed by CT. Uncoated data is from reference 20. (a) Room temperature. (b) 1316 °C.

From the CT images of impact tested EBC coated composites it is possible to determine the extent to which the projectile penetrated into the substrate. Figures 8(a) and (b) show the plot of the depth of penetration of projectile into the substrate with projectile velocity for EBC coated composite tested at mbient and at 1316 °C, respectively. For comparison purposes, the CT data of the uncoated composites tested under similar conditions are also included (ref. 20). The plot indicates that the uncoated and 225 µm EBC coated composites showed similar trends both at ambient temperature and at 1316 °C and that the depth of penetration of the projectile into the substrate for the uncoated and 225 µm EBC coated composites at a given velocity of projectile is measurably greater than that for the 525 µm EBC coated composites. This also suggests that thicker EBC coated composites reduce impact damage to the substrate more effectively than the thinner EBC due to better impact energy absorption mechanism in the thicker EBC. Also noticed in figures 8(a) and (b) is that at projectile velocities greater than 300 m/s for the uncoated and 225 µm EBC coated composites, the depth of damage is similar to the thickness of the specimens both at ambient and at 1316 °C whereas in 525 µm EBC coated composites at both test temperatures smaller amount of damage occurred within the coating. Therefore through the thickness damage to the substrate is limited.

Detailed examination of the craters and the surrounding damaged zone created by impact testing at ambient and at 1316 °C shows that at low projectile energy damage is limited to the surface coating. As the projectile velocity is increased a greater amount of damage to the coating is observed with sub-layers of the coating completely spalling off beyond a certain value of projectile velocity. The weakest spot in the multilayered EBC coating appears to be the interface between the silicon bond coat and intermediate coat which consists of a mixture of mullite and BSAS as shown in figure 9. The critical value of projectile energy for spalling depends on the EBC coating thickness and test temperature. For the composites coated with 225 µm EBC, spalling of sub-layer occurs at projectile velocity as low 160 m/s, but for the composites coated with 525 µm EBC it occurs at projectile velocity greater than 220 m/s. The coating damage appears to be slightly greater for the specimens tested at ambient temperature than that at 1316 °C. At projectile velocities greater than that required for spallation of EBC sub-layers, the damage is concentrated to the fiber ply under the EBC coating on the impacted side of the specimens. At velocities>300 m/s, the projectiles invariably perforated the substrate in the case of specimens coated with 225 µm EBC, but not in the specimens coated with 525 µm EBC.

To assess the influence of impact damage on tensile properties, the EBC coated specimens before and after impact tests were tensile tested at room temperature. Table I shows the in-plane tensile properties of the EBC coated MI SiC/SiC composite panels. A previous study has shown that within panel in-plane tensile properties MI SiC/SiC composites are not affected by EBC coating, but between panels significant variations in properties are observed due to batch to batch variations in constituents. Typical tensile stress-strain curves of impact tested MI SiC/SiC composite coated with 225 and 525 µm EBC are shown in figures 10(a) and (b), respectively. For comparison, the tensile stress-strain curve of an as-fabricated

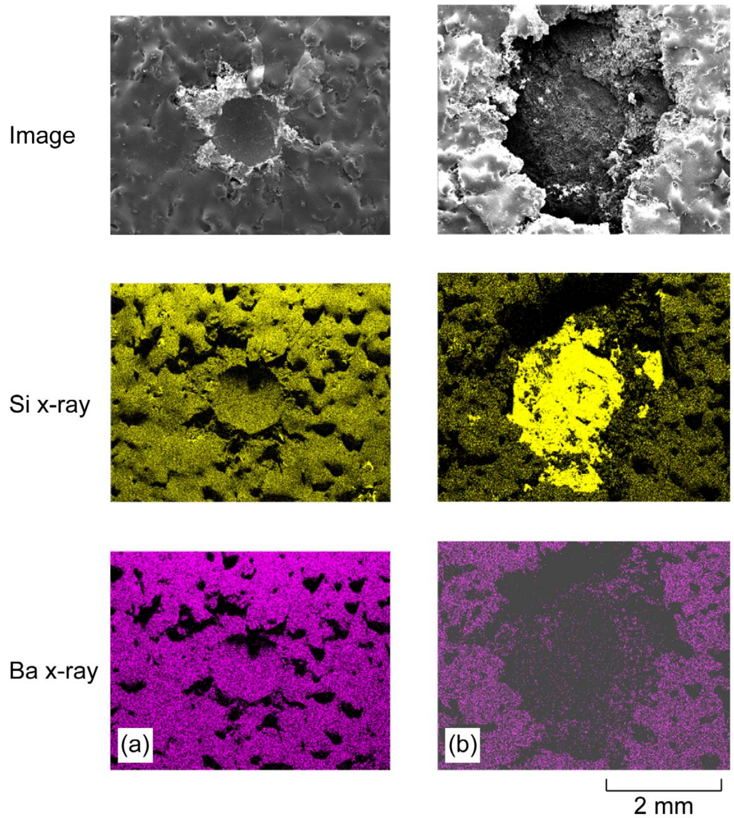

Figure 9.—SEM and elemental x-ray images of a 525 µm EBC coated SiC/SiC composite specimen impact tested at room temperature at two projectile velocities showing spallation of EBC at the silicon bond coat layer. (a) 160 m/s. (b) 220 m/s.

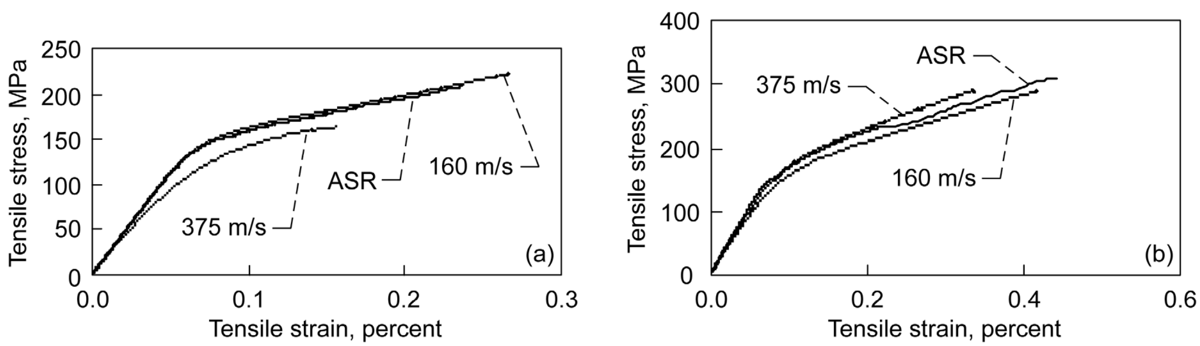

Figure 10.—Room temperature tensile stress-strain curve of EBC coated MI SiC/SiC composites after impact testing at room temperature showing influence of projectile velocity and EBC coating thickness. (a) 225 mm. (b) 525 mm.

TABLE I.—ROOM TEMPERATURE IN-PLANE TENSILE PROPERTIES OF EBC COATED 2-D WOVEN MI SIC/SIC COMPOSITES

Properties	MI SiC/SiC coated with 225 µm EBC	MI SiC/SiC coated with 525 µm EBC
Density (gm/cc)	2.81	2.91
Elastic modulus (GPa)	228	216
Deviation from linearity stress (MPa)	123	117
Deviation from linearity strain (%)	0.06	0.05
Ultimate tensile stress (MPa)	301	310
Ultimate tensile strain (%)	0.34	0.4

EBC coated MI SiC/SiC composite is included in these figures. In these figures the tensile stress-strain curve of specimens impact tested at 160 and 375 m/s were particularly chosen to reflect early and late stages of internal damage. In the early stages, the damage is limited only to EBC coating and in the late stage, damage extended deep into the substrate or sometimes perforation of the substrate occurs. Figure 10(a) shows that the stress-strain curve of 225 µm EBC coated specimens without impact and those impacted at 160 m/s is nearly the same, while those impacted at 375 m/s showed significant reduction in initial modulus (E), the stress corresponding to deviation from linearity (DFL), and the ultimate tensile strength (UTS). On the other hand, the stress-strain curves of MI SiC/SiC specimens coated with 525 µm EBC in as-fabricated condition and after impact testing at 160 and 375 m/s displayed similar features and no appreciable loss in E, DFL, and UTS from the baseline data. Comparison of figures 10(a) and (b) indicates a significant difference in UTS of MI SiC/SiC specimens coated with 225 and 525 µm EBC. This difference is not due to coating thickness difference, but due to the different vintage of panels.

To determine the effect of impact damage on tensile properties of the EBC coated composites accounting for batch to batch to variations in mechanical properties, it is necessary to normalize the data. Figures 11, 12, and 13 show influence of projectile velocity on normalized E, DFL stress, and UTS. For normalization, the tensile properties of the impact tested composites are divided by those of as-produced condition. For example, normalized E indicates ratio of E of the impact tested EBC coated specimens to the E of EBC coated specimens. In these figures the normalized data of impact tested MI SiC/SiC composites without EBC coating from reference 20 are also included. The following general statements can be deduced from these figures. First, the composites tested at projectile velocities up to 110 m/s show no significant loss in tensile properties compared to baseline tensile data for the as-produced EBC coated composites. Second, beyond 110 m/s, E, DFL, and UTS decrease linearly with increase in projectile velocity. Third, the E and DFL stress loss behaviors with increasing projectile velocity for the uncoated and EBC coated composites are similar. Fourth, the loss of UTS with increasing projectile velocity for the composite coated with 525 µm EBC is much lower than that observed for uncoated and 225 µm EBC coated composites. The loss of modulus and DFL stress indicates delamination of the fiber plies from the matrix and cracking of the matrix, where as loss of UTS indicates loss of load carrying capability of the composite due to loss of fiber as the projectile penetrates through the thickness. These plots also suggest that SiC/SiC composites coated with thicker EBC retain a greater percentage of the as-fabricated tensile properties after impact testing at velocities as high as 375 m/s compared to the uncoated SiC/SiC composites or similar composites coated with thinner EBC.

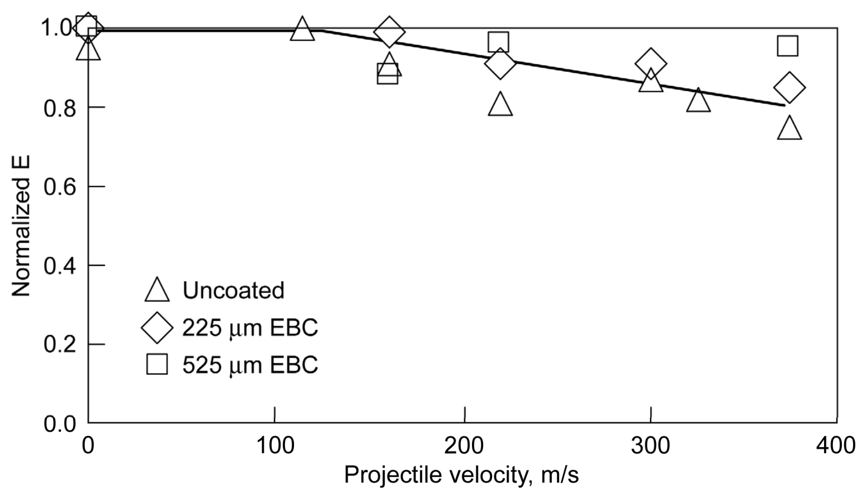

Figure 11.—Influence of projectile velocity on elastic modulus E for uncoated and EBC coated MI SiC/SiC composites impact tested at room temperature. Normalized E reflects ratio of the tensile modulus of impacted to un-impacted specimens. Uncoated data is from reference 20.

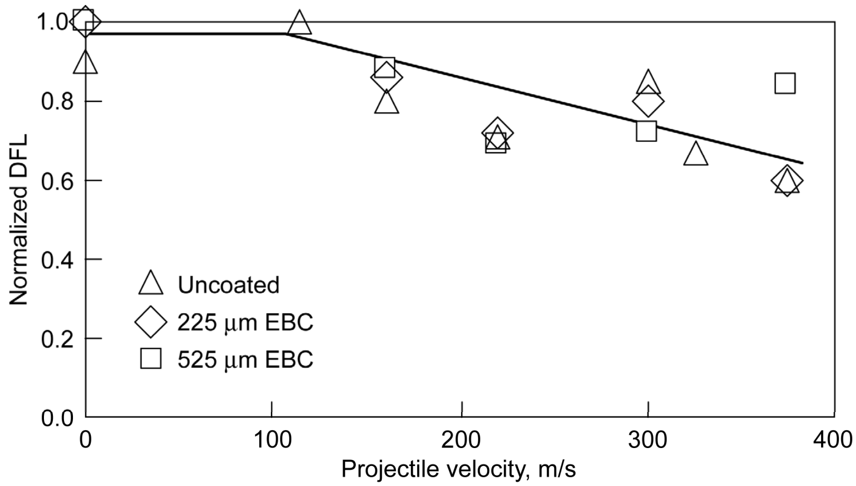

Figure 12.—Influence of projectile velocity on stress corresponding to DFL for uncoated and EBC coated MI SiC/SiC composites impact tested at room temperature. Normalized DFL reflects ratio of the DFL stress of impacted to un-impacted specimens. Uncoated data is from reference 20.

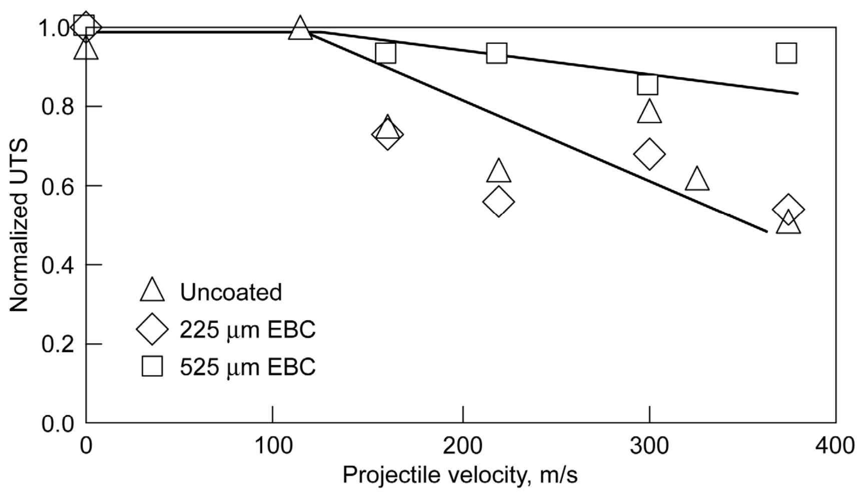

Figure 13.—Influence of projectile velocity on UTS for uncoated and EBC coated MI SiC/SiC composites impact tested at room temperature. Normalized UTS reflects ratio of the UTS of impacted to un-impacted specimens. Uncoated data is from reference 20.

Local damage or spallation of the EBC coating on MI SiC/SiC composite can lead to surface recession, internal oxidation, and mechanical property degradation. In this study the influence of oxidation on mechanical properties was not investigated because of the difficulty in gripping and aligning the EBC coated specimens in the tensile testing machine. A significant amount of thickness variation of the EBC coatings led to misalignment and premature failure of specimens due to bending strain. Also in some instances the coating crushed within the grip. Therefore, only effects of impact damage on internal oxidation were investigated in this study. For this purpose, composite specimens of dimensions 45- by 8- by 2-mm were coated on all sides with 525 µm thick EBC and impact tested at 220 and 290 m/s at ambient temperature to cause local damage or spalling of EBC. These specimens were then exposed to a flowing gas mixture of 0.1 MPa 90 percent H_2O+10 percent O_2 at 1316 °C for 500 hr. Following oxidation exposure, the specimen was sectioned at the spalled spot, mounted in a mold, infiltrated with epoxy and polished using standard metallographic procedures. Figure 14 shows a SEM micrograph of a

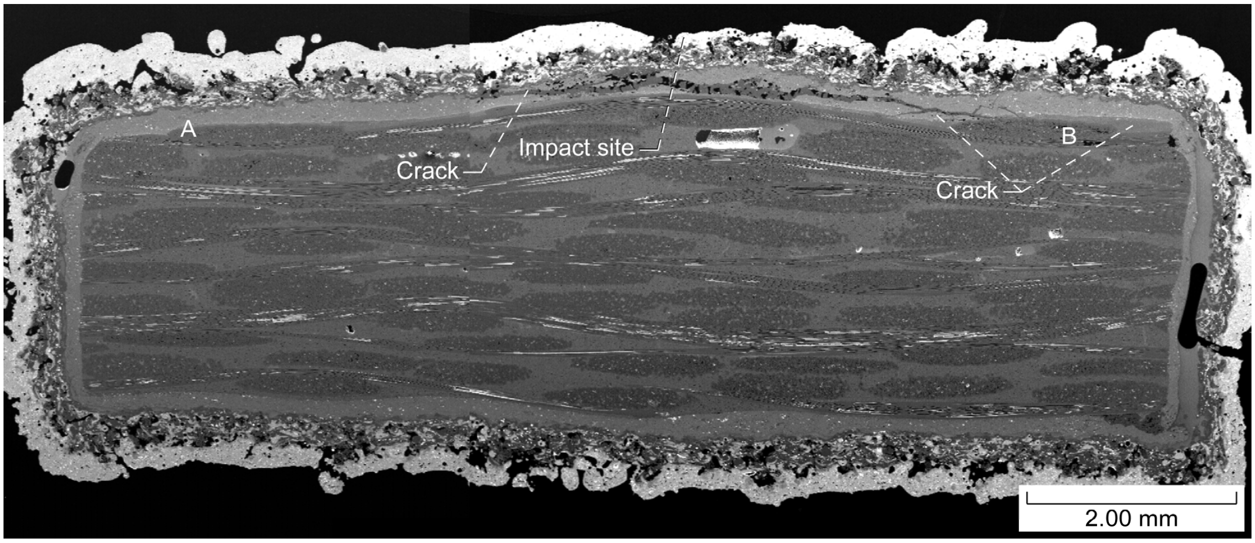

Figure 14.—SEM image of cross section of 525 µm thick EBC coated MI SiC/SiC composite impact tested at room temperature at 220 m/s and then oxidized at 1316 °C for 500 hr in 0.1 MPa flowing gas mixture of 90 percent H_2O + 10 percent O_2 showing extent of internal oxidation from cracks formed below impacted site.

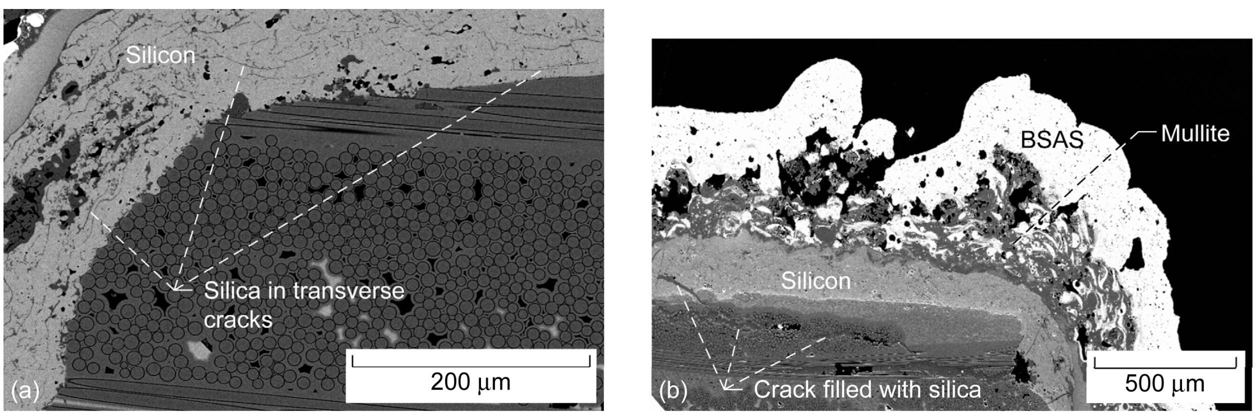

Figure 15.—High magnification SEM photographs of regions A and B from figure 14. (a) No silica growth is seen in undamaged areas. (b) Silica formation is seen in areas where cracks are formed in substrate.

cross-section of a specimen impact tested at 220 m/s. In this figure, the impacted site and the crack created by the projectile after impact are also shown, but the bottom of the crater is not visible because the specimen was sectioned at the rim of the crater. The crack under the impact site starts at the interface between the silicon bond coat and the intermediate coat, and progresses into the silicon bond coat and then into the first fiber ply of the substrate. The oval cavity in the EBC coating (on right side of the specimen at the mid region in figure 14) probably existed before oxidation exposure due to poor adherence of EBC on the sides of specimen, but the large crack in the EBC coating on the cavity wall was probably formed during cool down after oxidation run. Non uniform coverage of plasma sprayed EBC on the cut ends and thin sections may have contributed to the formation of these defects. To determine the extant of oxidation into the substrate via uncracked and cracked regions of EBC coating as well as via delamination created by impact testing various regions of the oxidized specimen were examined. In figure 14, the region A represents an uncracked region below the EBC coating and the region B represents cracked region. A high magnification photograph of region A indicates the following: formation of silica in transverse cracks of the silicon bond; minimal silica growth between the silicon bond coat and the substrate, and within the axial and transverse fiber plies (fig. 15(a)). On the other hand in region B, the delamination cracks were filled with silica and acted as a conduit for internal oxidation of the substrate (fig. 15(b)).

Figure 16 shows a SEM micrograph of a cross-section of a specimen oxidized at 1316 °C for 500 hr in a moisture environment after impact testing at 290 m/s. In this figure, the crater formed in the EBC coating (area A in figure 16) and crack between last ply of the substrate and the EBC coating (area B in figure 16) are clearly visible. The crater in the coating in the mid section and the delaminated area between the coating and the substrate at bottom of the figure is caused by impact testing. Observation of a region slightly under the impact crater at higher magnification indicates a hairline crack filled with silica in the transverse fiber ply (fig. 17). This crack extended across the specimen. Silica growth is also observed in the crack at the bottom end of the specimen as well as other hairline cracks formed within the substrate adjacent to the EBC coating.

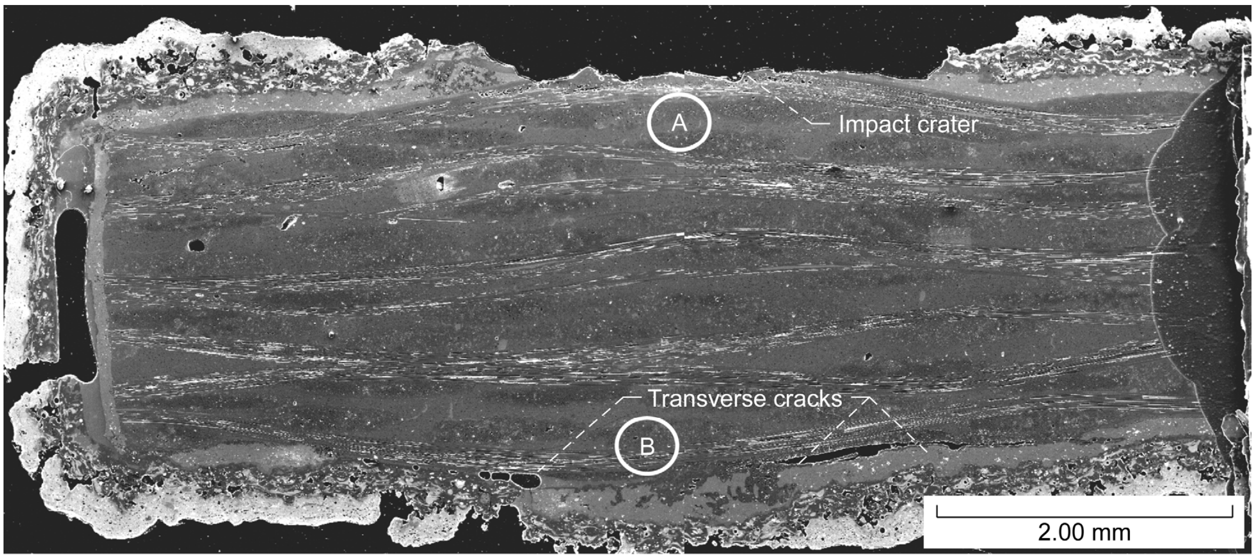

Figure 16.—SEM image of cross section of impact tested MI SiC/SiC composite coated with 525 μm thick EBC showing defects created by impact and regions of specimen further analyzed for oxidation damage. Specimen impact tested at 290 m/s and then oxidized at 1316 °C for 500 hr in flowing gas mixture of 0.1 MPa 90 percent H_2O + 10 percent O_2.

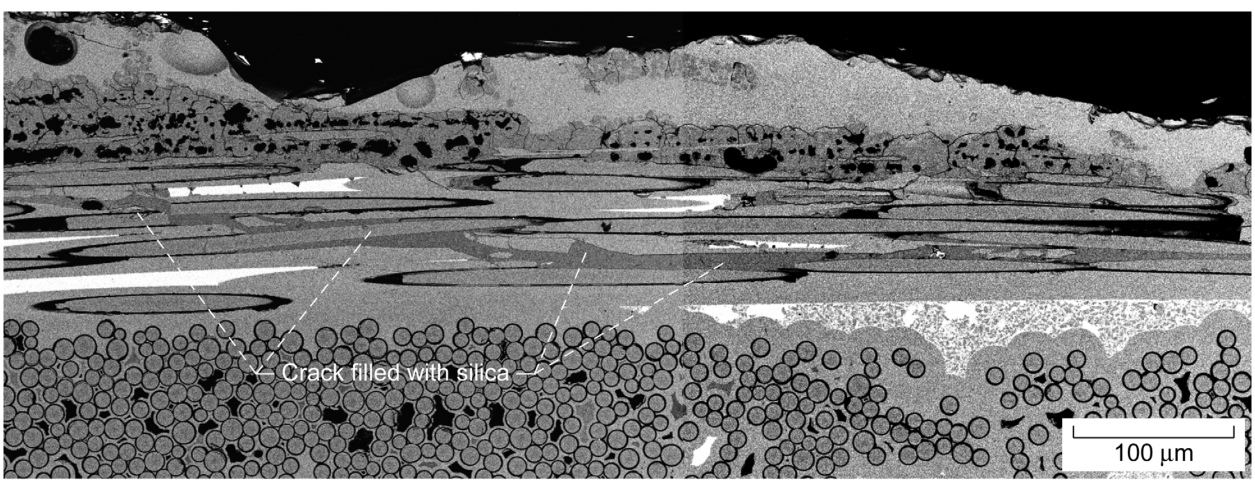

Figure 17.—High magnification SEM photograph of an area below impact crater in figure 16 (region A) showing silica growth within the transverse tow where cracks are formed by impact.

4. Discussion

In this study the influence of EBC coating thickness on stability and performance of MI SiC/SiC composites under impact conditions was studied. Different thicknesses of EBC coating are required in different areas of the components because of significant thickness variations in the leading to trailing edges of nozzles and blades. Results indicate that impact damage starts with coating damage and then progresses into the substrate. At early stages, the sub-layers of EBC coating debonded and spalled off at projectile velocities greater than 160 m/s. The weakest link in the EBC coating is the interface between the intermediate coat (a mixture of mullite and BSAS) and the silicon bond coat. In addition to coating damage, internal damage within the substrate in the form of fiber ply delamination close to the impacted site was observed. As the projectile velocity increases delamination of the fiber ply on the back side of the specimen occurs. Delamination in the EBC sub-layers as well as between the fiber ply and the SiC matrix is due to poor through-the-thickness bonding. The low inter-laminar tensile strength of 2-D woven MI SiC/SiC composites is an indication of poor bonding in the through-the-thickness direction. The impact tested SiC/SiC composite coated with thicker EBC appears to shield substrate damage and retain a greater percentage of as produced in-plane tensile properties compared to those coated with thin EBC. The impact test temperature had minimal effect. At a given projectile velocity, the depth and width of the damage zone are nearly the same suggesting that thin EBC coatings are not effective in shielding substrate damage. Exposure of the delaminated impact tested specimen in the moisture environment shows growth of silica in the cracks and in the region where EBC is damaged.

Pulsed thermography and computed tomography were utilized to evaluate impact damage in the EBC coated MI SiC/SiC composites. From the coated and uncoated sides of the samples in this study, thermography was able to detect cracks or delamination at the interface of the EBC and the substrate. Delamination very near the back surface of the substrate material was not detected from the coated side of the sample but was easily detected from the uncoated back side. This was expected as defects and flat bottom holes very near the back surface of uncoated samples were also difficult to detect (ref. 18). The cooling behavior can be monitored to qualitatively describe the location of damage within the thickness of these material systems. Some advantages of using pulsed thermography are that it is a full field, non contact method that requires access to a single side of a component. In addition, damage can be further quantified and classified with a calibration standard having seeded defects in the coating, the substrate, and at the coating substrate interface. Delamination locations and profiles were evident in the CT images. CT has the distinct advantage of providing a cross sectional view of a component. However, CT has significant disadvantages with respect to inspection time and costs. In addition, component size often needs to be limited.

5. Summary of Results

Impact resistance of 2-D woven MI SiC/SiC composites coated with 225 and 525 μm thick EBC were investigated at room temperature and at 1316 °C. The impact tests were performed using 1.59-mm diameter hardened steel projectiles at projectile velocities up to 400 m/s. Damage evolution in the EBC coating and within the substrate with projectile velocity was monitored with SEM, pulsed thermography, and computed tomography. Residual tensile properties of impact tested specimens were measured at room temperature and 1316 °C. To assess extent of oxidation by recession, some impact tested specimens were exposed to a mixture of 0.1 MPa 90 percent H_2O+10 percent O_2 at 1316 °C for 500 hr. Key findings are the following

(a) Damage to EBC coating occurs at projectile velocities greater than 160 m/s. The weakest link in the coating is the interface between silicon bond coat and the intermediate coat consisting of a mixture of mullite and BSAS.

(b) At all tested projectile velocities, the MI SiC/SiC composites coated with 525 μm EBC show less damage to the substrate compared to those coated with 225 μm.

(c) Impact behavior of uncoated SiC/SiC composites and those coated with 225 μm EBC are similar.
(d) At any fixed projectile velocity beyond 120 m/s, the retained modulus and matrix cracking stress values for the impacted tested uncoated and EBC coated MI SiC/SiC composites are nearly the same within the experimental accuracy, but retained UTS values for the impact tested 525 μm EBC coated MI SiC/SiC composites are measurably higher than those of the other two groups.
(e) Impact induced delamination cracks in the substrate act as conduits for surface recession by oxidation in a moisture environment.

6. Conclusion

Debonding of the EBC coating and the fiber plies in the substrate due to single particle impact are the major concern affecting long term durability of the composites. To avoid the debonding within the EBC sub layers, EBC needs to be toughened by particulate or whisker reinforcement. On the other hand debonding the fiber plies within the substrate can be reduced or avoided by changing the fiber architecture from 2-D woven to 3-D orthogonal or 2.5-D angle interlock configuration.

References

1. D. Brewer, *Mat. Sci. and Eng*., A261, pp. 284–291, (1999).
2. E.A. Gulbransen and S.A. Jansson, "The High-Temperature Oxidation, Reduction, and Volatilization Reactions of Silicon ad Silicon Carbide," *Oxidation of Metals*, 4 [3] pp. 181–201, (1972).
3. P.J. Jorgensen, M.E. Wadsworth, and I.B. Cutler, "Oxidation of Silicon Carbide," *J. Am. Ceram. Soc*., 42 (12): pp. 613–616 (1959).
4. R.C. Robinson and J.L. Smialek, *J. Am. Ceram. Soc.,* 82 (7): pp. 1817–1825, 1999.
5. E.J. Opila, J.A. Smialek, R.C. Robinson, D.S. Fox, and N.S. Jacobson, *J. Am. Ceram. Soc.,* 82 (7): pp. 1826–1834, 1999.
6. K.N. Lee, *Surface Coating Technology*, pp. 133–134, 1–7, 2000.
7. K.N. Lee, D.S. Fox, J.I. Eldridge, D. Zhu, R.C. Robinson, N.P. Bansal, and R.A. Miller, *J. Am. Ceram. Soc*., 86 (8): pp. 1299–1306, 2003.
8. K.N. Lee, D.S. Fox, and N.P. Bansal, "Rare earth silicate environmental barrier coatings for SiC/SiC composites and Si_3N_4 ceramics," *J. Eur. Ceram. Soc.*, 25 (10): pp. 1705–1715, 2005.
9. R.T. Bhatt, G.N. Morscher, and K.N. Lee, "Influence of EBC Coating on Tensile Properties of MI SiC/SiC Composites," Proceedings of PACRIM conference, 2005.
10. G.S. Corman, A.J. Dean, S. Brabetz, M.K. Brun, K.L. Luthra, L. Tognarelli, and M. Pecchioli, "Rig and engine testing of melt infiltrated ceramic composites for combustor and shroud applications," *J. Eng. Gas Tur. and Pow.*-Transactions of the ASME 124 (3): pp. 459–464 JUL 2002.
11. N. Miriyala, J. Kimmel, J. Price, K. More, P. Tortorelli, H. Eaton, G. Linsey, and E. Sun, "The Evaluation of CFCC Liners after Field Testing in a Gas Turbine-III," ASME paper no. GT2002–30585, (2002).
12. Y. Furuse, T. Teramae, T. Tsuchiya, F. Maeda, Y. Tsukuda, and K. Wada, "Application of Ceramics to a Power Generating Gas Turbine," Ceramic Gas Turbine design and Test Experience-Progress in Ceramic Gas Turbine Development, V 1, eds M van Roode, M.K. Ferber, and D.W. Richerson, The American Society of Mechanical Engineers, Three Parks Avenue, New York, NY 10016, 2002.
13. A.F. Dericioglu, S. Zhu, Y. Kagawa, and H. Kasano, "Damage Behavior of Air- Plasma-Sprayed Thermal Barrier Coatings under Foreign Object Impact," *Advanced Engineering Materials*, 5 [10] pp. 735–737, 2003.
14. X. Chen, R. Wang, N. Yao, A.G. Evans, J.W. Hutchinson, and R.W. Bruce, "Foreign object damage in a thermal barrier system: mechanisms and simulations," *Mater. Sci. Eng.* A 352, pp. 221, 2003.
15. S.K. Lau, S.J. Calandra, and R.W. Ohnsorg, U.S. Patent no. 5,840,221, (1998).

16. K.N. Lee, R.A. Miller, and N.S. Jacobson, "New Generation of Plasma-Sprayed Mullite Coatings on Silicon-Carbide," *J. Am. Ceram. Soc.* 78 (3) pp. 705–710 (1995).
17. S.R. Choi, J.M. Pereira, L.A. Janosik, and R.T. Bhatt, *Ceram. Eng. Sci. Proc*., 23[3] pp. 193–202 (2002).
18. L.M. Cosgriff, R.T. Bhatt, S.R. Choi, and D.S. Fox, "Thermographic characterization of impact damage in SiC/SiC composite materials," *Proc. SPIE*, 5767, pp. 363–372, 2005.
19. P.O. Moore, ed. Nondestructive Testing Handbook Radiographic Testing vol. 4, 3rd ed., Columbus: American Society for Nondestructive Testing, Inc, 2002.
20. R.T. Bhatt, S. R. Choi, L.M. Cosgriff, D. Fox, and K.N. Lee, "Impact Damage Resistance of Uncoated MI SiC/SiC Composites" to be published.

REPORT DOCUMENTATION PAGE				*Form Approved OMB No. 0704-0188*

1. REPORT DATE *(DD-MM-YYYY)*
01-10-2008

2. REPORT TYPE
Technical Memorandum

3. DATES COVERED *(From - To)*

4. TITLE AND SUBTITLE
Impact Resistance of EBC Coated SiC/SiC Composites

5a. CONTRACT NUMBER

5b. GRANT NUMBER

5c. PROGRAM ELEMENT NUMBER

6. AUTHOR(S)
Bhatt, Ramakrishna, T.; Choi, Sung, R.; Cosgriff, Laura, M.; Fox, Dennis, S.; Lee, Kang, N.

5d. PROJECT NUMBER

5e. TASK NUMBER

5f. WORK UNIT NUMBER
WBS 561581.02.08.03

7. PERFORMING ORGANIZATION NAME(S) AND ADDRESS(ES)
National Aeronautics and Space Administration
John H. Glenn Research Center at Lewis Field
Cleveland, Ohio 44135-3191

8. PERFORMING ORGANIZATION REPORT NUMBER
E-15685

9. SPONSORING/MONITORING AGENCY NAME(S) AND ADDRESS(ES)
National Aeronautics and Space Administration
Washington, DC 20546-0001
and
U.S. Army Research Laboratory
Adelphi, Maryland 20783-1145

10. SPONSORING/MONITORS ACRONYM(S)
NASA; ARL

11. SPONSORING/MONITORING REPORT NUMBER
NASA/TM-2008-214406; ARL-TR-0646

12. DISTRIBUTION/AVAILABILITY STATEMENT
Unclassified-Unlimited
Subject Category: 27
This publication is available from the NASA Center for AeroSpace Information, 301-621-0390

13. SUPPLEMENTARY NOTES

14. ABSTRACT
Impact performance of 2-D woven SiC/SiC composites coated with 225 and 525 μm thick environmental barrier coating (EBC) was investigated. The composites were fabricated by melt infiltration and the EBC was deposited by plasma spray. Impact tests were conducted at room temperature and at 1316 °C in air using 1.59-mm diameter steel-balls at projectile velocities ranging from 110 to 375 m/s. Both microscopy and nondestructive evaluation (NDE) methods were used to determine the extent of damage in the substrate and coating with increasing projectile velocity. The impacted specimens were tensile tested at room temperature to determine their residual mechanical properties. At projectile velocities less than 125 m/s, no detectable damage was noticed in the MI SiC/SiC composites coated with 525 μm EBC. With increase in projectile velocity beyond this value, spallation of EBC layers, delamination of fiber plies, and fiber fracture were detected. At a fixed projectile velocity, the composites coated with 525 μm EBC showed less damage than the composite coated with 225 μm EBC. Both types of EBC coated composites retained a large fraction of the baseline properties of as-fabricated composites and exhibited non-brittle failure after impact testing at projectile velocities up to 375 m/s. Exposure of impact tested specimens in a moisture environment at 1316 °C for 500 hr indicated that the through-the-thickness cracks in the EBC coating and delamination cracks in the substrate generated after impact testing acted as conduits for internal oxidation.

15. SUBJECT TERMS
SiC/SiC composites; Impact; EBC coating; Microstructure; Mechanical Properties; NDE

16. SECURITY CLASSIFICATION OF:			17. LIMITATION OF ABSTRACT	18. NUMBER OF PAGES	19a. NAME OF RESPONSIBLE PERSON
a. REPORT	b. ABSTRACT	c. THIS PAGE			STI Help Desk (email:help@sti.nasa.gov)
U	U	U	UU	22	19b. TELEPHONE NUMBER *(include area code)* 301-621-0390